CHARACTERIZATION OF NON-SYMMETRICAL DAMAGE IN SMART PLATE-LIKE STRUCTURES

H.T. Banks and P. Emeric

Center for Research in Scientific Computation
North Carolina State University
Raleigh, NC 27695-8205

INTRODUCTION

Smart material technology is an active area of research, with promising applications that include, for instance, control systems [2, 8] and nondestructive evaluation [3, 8]. Among the different types of smart material structures currently studied, structures with bonded piezoelectric ceramic patches are of particular interest [6]. When an electric field is applied, piezoceramic patches induce strains in the material to which they are bonded and, conversely, they produce a voltage when a deformation occurs in the material [7, 8]. As a consequence, these patches can act both as actuators and sensors, providing the host structure with smart material capabilities.

Previous work concerned the characterization of symmetrical damage in beams by identification of the physical parameters [4]. The focus of this study is the characterization of non-symmetrical damage in partially clamped plate-like structures. In the first part, a two-dimensional model for the in-plane vibrations of such structures is proposed. In the second part, an experimental setup to determine the time resolved vibration response of damaged Aluminum plate-like structures is described. The experimental data is compared to numerical experiments.

MODEL

Fig. 1 depicts a cross section Ω of the clamped plate-like structure with a non-symmetrical damage. Γ is the boundary with no displacement. Motion is assumed to be longitudinal (in the x direction) and transverse (in the y direction). A groove in the z direction represents the defect. Piezoelectric patches, noted Ω_{pe}, are symmetrically bonded to the upper and lower surfaces. The region $\Omega_B = \Omega \cup \Omega_{pe}$

Review of Progress in Quantitative Nondestructive Evaluation, Vol. 17
Edited by D.O. Thompson and D.E. Chimenti,, Plenum Press, New York, 1998

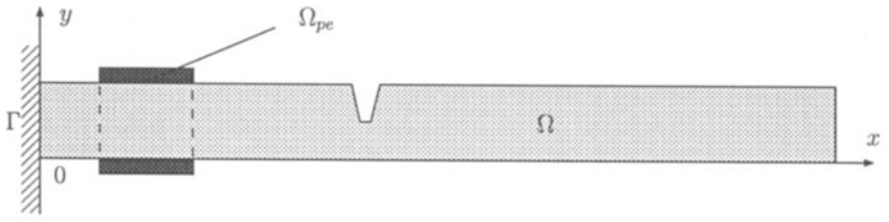

Figure 1. Cross section of a cantilever plate-like structure.

is the complete structure. The motion of the structure in the (x, y) plane cannot be modeled accurately by classical thin beam or thin plate models. Such models assume a shell coordinate system with an unperturbed middle surface as the reference surface. The presence of non-symmetrical damage introduces a coupling of the motions in the (x, y) plane which is not taken into account by these models. We model this coupled motion assuming a state of plane strain in the structure; that is, away from the edges, no displacement takes place in the z direction.

Strong Form of the Equations of Motion

We combine force balancing with constitutive hypotheses to obtain the equations of motion for the displacements U and V in the x and y directions, respectively [5]. We obtain

$$\begin{cases} \hat{\rho}\ddot{U} = & \dfrac{\hat{E}}{1+\hat{\nu}}\left(\dfrac{1-\hat{\nu}}{1-2\hat{\nu}}U_{,xx} + \dfrac{1}{2}U_{,yy} + \dfrac{1}{2(1-2\hat{\nu})}V_{,xy}\right) \\ & + \dfrac{\hat{C}_D}{1+\hat{\nu}}\left(\dfrac{1-\hat{\nu}}{1-2\hat{\nu}}\dot{U}_{,xx} + \dfrac{1}{2}\dot{U}_{,yy} + \dfrac{1}{2(1-2\hat{\nu})}\dot{V}_{,xy}\right) + \dfrac{q_x}{b} \\ \hat{\rho}\ddot{V} = & \dfrac{\hat{E}}{1+\hat{\nu}}\left(\dfrac{1-\hat{\nu}}{1-2\hat{\nu}}V_{,yy} + \dfrac{1}{2}V_{,xx} + \dfrac{1}{2(1-2\hat{\nu})}U_{,xy}\right) \\ & + \dfrac{\hat{C}_D}{1+\hat{\nu}}\left(\dfrac{1-\hat{\nu}}{1-2\hat{\nu}}\dot{V}_{,yy} + \dfrac{1}{2}\dot{V}_{,xx} + \dfrac{1}{2(1-2\hat{\nu})}\dot{U}_{,xy}\right) + \dfrac{q_y}{b} \end{cases} \tag{1}$$

where q_x and q_y are the horizontal and vertical components of an external force/unit area acting on the element[1]. $\ddot{U}$ and $\ddot{V}$ are the second time derivatives of the displacements U and V. Here, $\hat{\rho} > 0$ is the mass per unit volume, $\hat{C}_D > 0$ is a damping coefficient, $\hat{E} > 0$ is Young's modulus and $0 \leq \hat{\nu} < 1/2$ is Poisson's ratio. These are locally constant material properties with definitions:

$$\begin{aligned} \hat{\rho} &= \rho\chi_\Omega + \rho_{pe}\chi_{\Omega_{pe}}, & \hat{\nu} &= \nu\chi_\Omega + \nu_{pe}\chi_{\Omega_{pe}} \\ \hat{C}_D &= C_D\chi_\Omega + C_{Dpe}\chi_{\Omega_{pe}}, & \hat{E} &= E\chi_\Omega + E_{pe}\chi_{\Omega_{pe}}, \end{aligned} \tag{2}$$

where the subscript $_{pe}$ indicates the value for the piezoelectric patches. The

[1]Typically, subscripts such as those above do not represent derivatives; for partial derivatives, we shall use either $\frac{\partial U}{\partial x}$ or $U_{,x}$ whereas q_x will denote the x component of the force q.

functions χ_Ω and $\chi_{\Omega_{pe}}$ are characteristic functions with definition

$$\chi_\Omega = \begin{cases} 1 & in\,\Omega \\ 0 & otherwise \end{cases} \quad and \quad \chi_{\Omega_{pe}} = \begin{cases} 1 & in\,\Omega_{pe} \\ 0 & otherwise. \end{cases} \tag{3}$$

Boundary and Initial Conditions

For the clamped end, there are no in-plane displacements at any time. These boundary conditions are written:

$$U(t,0,y) = 0, \quad V(t,0,y) = 0. \tag{4}$$

All other boundaries are free of surface traction. By using Cauchy's formula, this condition can be written as:

$$\begin{pmatrix} \sigma_x & \tau_{xy} \\ \tau_{xy} & \sigma_y \end{pmatrix} \begin{pmatrix} n_x \\ n_y \end{pmatrix} = 0. \tag{5}$$

where σ_x, σ_y and τ_{xy} are the horizontal, vertical and shear stresses. n_x and n_y are the components of a unit outer normal surface vector along the boundary.

The initial conditions characterize the displacement and velocity at every point of the structure at $t = 0$. These are assumed to be given by:

$$\begin{aligned} U(0,x,y) &= U_0(x,y), \quad V(0,x,y) = V_0(x,y), \\ \dot{U}(0,x,y) &= U_1(x,y), \quad \dot{V}(0,x,y) = V_1(x,y), \end{aligned} \quad \text{for } (x,y) \in \Omega_{\mathcal{B}} \tag{6}$$

Weak Form of the Equations

The weak form of the equations of motion can be found by integration by parts of the strong form. For a complete derivation, see [5]. The weak formulation is:

$$\begin{cases} \int_{\Omega_{\mathcal{B}}} \hat{\rho}\ddot{U}\phi_1 = \int_{\Omega_{\mathcal{B}}} \frac{q_x}{b}\phi_1 \\ - \int_{\Omega_{\mathcal{B}}} \tilde{E}(2-2\hat{\nu})U_{,x}\phi_{1,x} - \int_{\Omega_{\mathcal{B}}} \tilde{E}(1-2\hat{\nu})(U_{,y}+V_{,x})\phi_{1,y} - 2\int_{\Omega_{\mathcal{B}}} \tilde{E}\hat{\nu}V_{,y}\phi_{1,x} \\ - \int_{\Omega_{\mathcal{B}}} \tilde{C}_D(2-2\hat{\nu})\dot{U}_{,x}\phi_{1,x} - \int_{\Omega_{\mathcal{B}}} \tilde{C}_D(1-2\hat{\nu})(\dot{U}_{,y}+\dot{V}_{,x})\phi_{1,y} - 2\int_{\Omega_{\mathcal{B}}} \tilde{C}_D\hat{\nu}\dot{V}_{,y}\phi_{1,x} \\ \int_{\Omega_{\mathcal{B}}} \hat{\rho}\ddot{V}\phi_2 = \int_{\Omega_{\mathcal{B}}} \frac{q_y}{b}\phi_2 \\ - \int_{\Omega_{\mathcal{B}}} \tilde{E}(2-2\hat{\nu})V_{,y}\phi_{2,y} - \int_{\Omega_{\mathcal{B}}} \tilde{E}(1-2\hat{\nu})(U_{,y}+V_{,x})\phi_{2,x} - 2\int_{\Omega_{\mathcal{B}}} \tilde{E}\hat{\nu}U_{,x}\phi_{2,y} \\ - \int_{\Omega_{\mathcal{B}}} \tilde{C}_D(2-2\hat{\nu})\dot{V}_{,y}\phi_{2,y} - \int_{\Omega_{\mathcal{B}}} \tilde{C}_D(1-2\hat{\nu})(\dot{U}_{,y}+\dot{V}_{,x})\phi_{2,x} - 2\int_{\Omega_{\mathcal{B}}} \tilde{C}_D\hat{\nu}\dot{U}_{,x}\phi_{2,y} \end{cases} \tag{7}$$

for all sufficiently smooth ϕ_1 and ϕ_2 satisfying $\phi_1 = \phi_2 = 0$ on Γ.

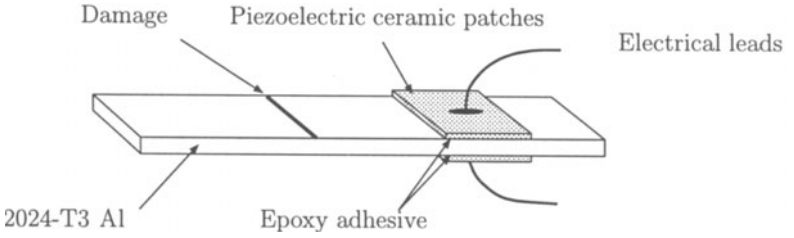

Figure 2. Beam with bonded piezoelectric ceramic patches.

Applied Forces

The forces induced in the structure when a voltage is applied to the piezoelectric patches can be very irregular. The corresponding model and a mathematical formulation of the problem as a second order equation in time, detailed in [1], allow the discussion of existence and uniqueness of the solutions and their continuity with respect to the data. The general input forces due to the patches allow well-posedness for the weak form of the equations in the case of strong damping. A Galerkin method was used with linear splines for the approximation of the dynamics of the structure. Numerical simulations are compared with the experimental data in the next section.

EXPERIMENTS

Specimens: Description and Preparation

A series of experiments were conducted to determine the time resolved vibrational response of cantilever structures described in Fig. 1. As depicted in Fig. 2, piezoelectric ceramic patches were symmetrically bonded to each side of aluminum plates. This arrangement allowed pure bending of the structure by exciting the patches out of phase. The structures consisted of $304.8 \times 25.4 \times 1.016$ mm 2024-T3 Aluminum slabs. The patches were $25.4 \times 25.4 \times 0.0508$ mm. lead zirconate titanates, appropriate for large displacement applications. Both Aluminum and ceramic surfaces were lightly sanded to roughen their surfaces and cleaned with trichloroethane. They were bonded with a low viscosity, room temperature cure epoxy adhesive. Electrical leads were soldered on the outside surface of the patches. The damage was simulated by machining a 1.524 mm wide groove as depicted in Fig. 2.

Experimental Setup

Fig. 3 depicts a diagram of the experimental setup used to determine the time resolved vibrational response of plate-like structures. A function generator provided the excitation to the patches. The piezoelectric patches were excited with a 2 ms square pulse signal. An oscilloscope was used to digitize the electrical signal generated by the deformation of the structure. A set of diodes, acting as a switch, was used to allow the input signal to the patches and their electrical response to the oscilloscope without interference. A personal computer allowed the storage of the data for further processing.

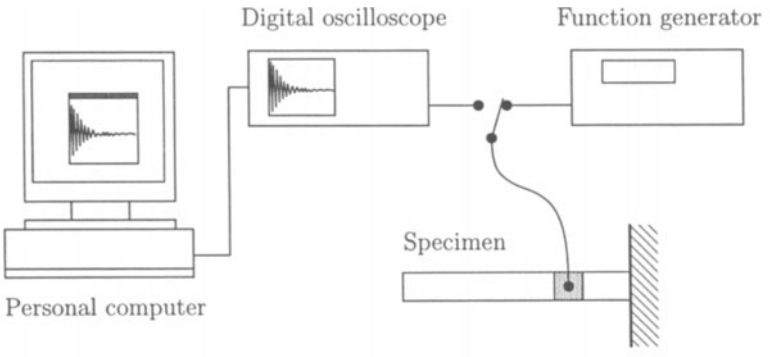

Figure 3: Experimental setup.

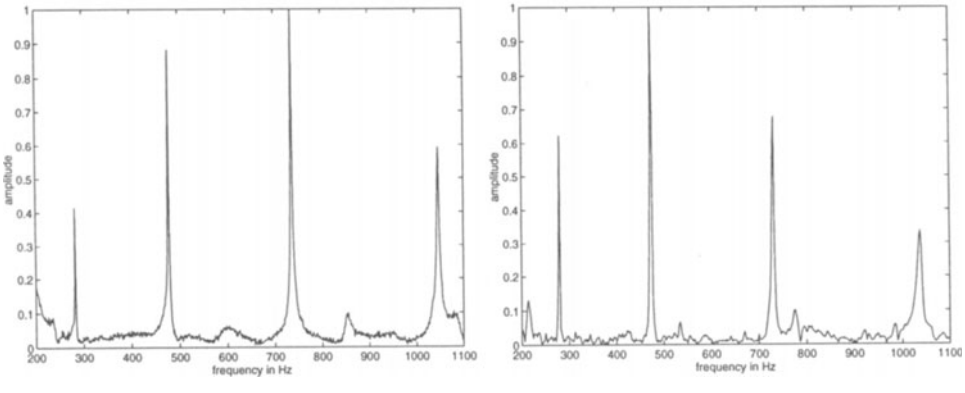

Figure 4. Normalized frequency spectrum responses of structure #5 to patch excitation(left) and hammer hit (right).

Results and Discussions

The results obtained by using the patches in self actuator/sensing mode were confirmed by experiments conducted in the passive sensing mode with excitations provided by hammer hits. Structure #5 was excited by hammer hits and let free to vibrate. The data was collected after each hit. Vibration data was also collected when the excitation was provided by the piezoelectric patches. Fig. 4 shows the frequency spectrum of typical data sets. The peaks correspond to the natural frequencies of the structure. The frequency spectrum for both types of excitation, passive and smart sensing, are similar.

To evaluate the influence of changes in the clamping strength and position, a structure was released and re-clamped in position between each data acquisition. The same repeated experiments were conducted with the structure left clamped at all times. Fig. 5 shows the data collected for structure #8. 5 sets are displayed for both graphs. An excellent agreement is found for the positions of the natural frequency peaks visible on both graphs.

To characterize the damage detection capabilities of the smart sensing

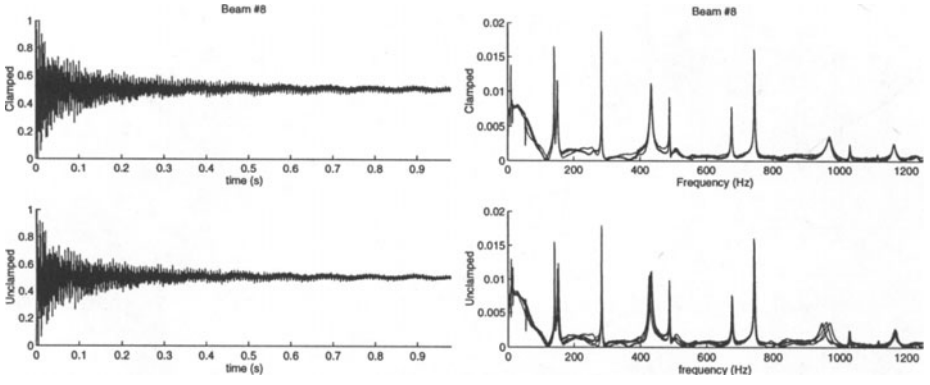

Figure 5. Time domain and frequency data for structure #8 for release/re-clamp test (bottom) and for clamped test (top).

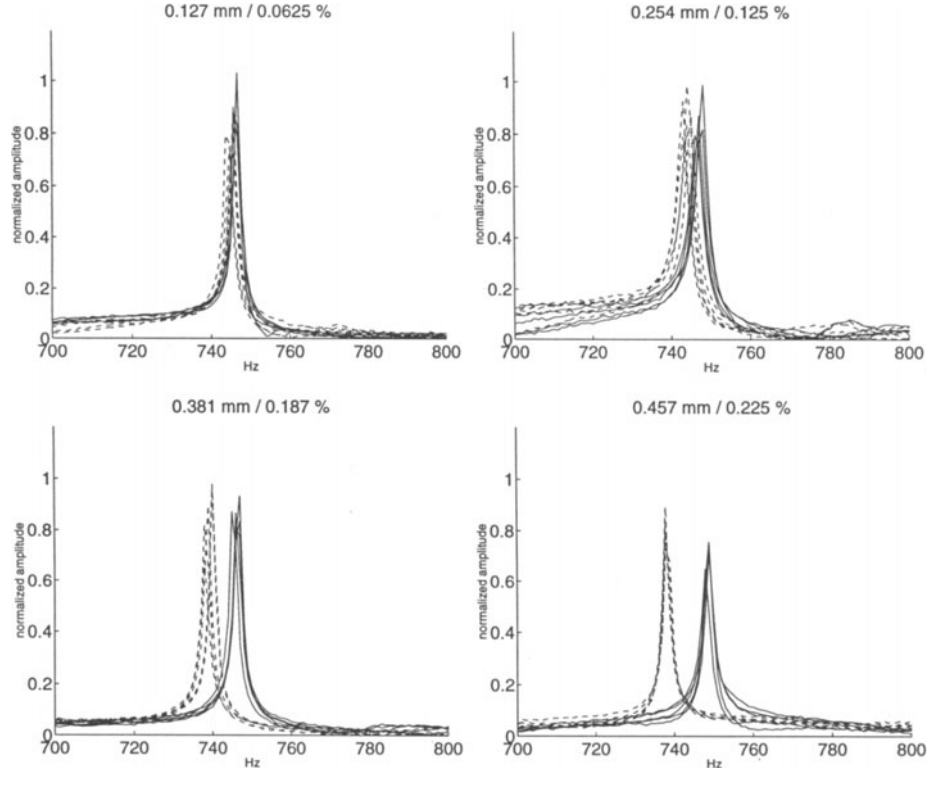

Figure 6. Frequency shifts due to damage. The depth of the groove and the total mass loss (in %) are indicated at the top of the graphs.

method, several structures were damaged by machining 1.524 mm wide grooves of various depths located 38.10 mm from the patches. Fig. 6 shows the shifts of a

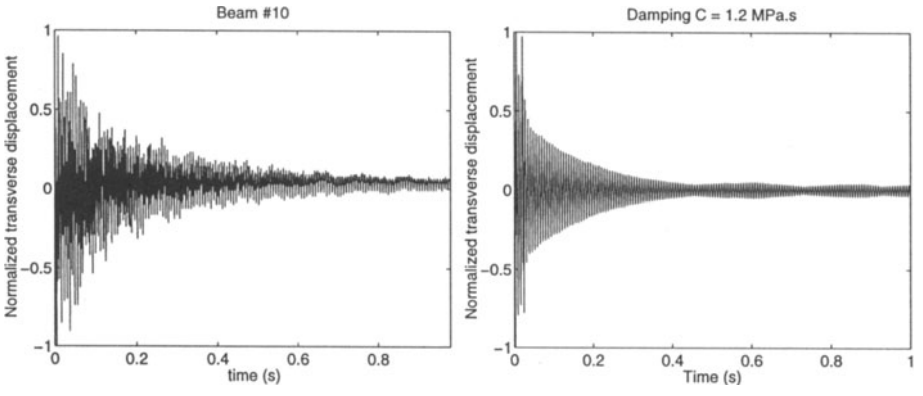

Figure 7. Experimental (left) and simulated time domain vibration responses (right).

natural frequency as the depth of a defect increases. The experiments were repeated five times by releasing the structure between each data acquisition.

Fig. 7 allows one to compare experimental data with simulated data obtained from the finite element model. The material properties for aluminum used in the simulation were $E = 7.3\ 10^{10}\ Pa$, $\rho = 2770\ kg/m^3$, $\nu = 0.33$ and $C_D = 1.2\ MPa.s$.

CONCLUSION

A two-dimensional model for a non-symmetrically damaged clamped plate-like structure was presented.

An experimental setup was built to allow the acquisition of time resolved vibration data. The results obtained in the passive and smart sensing modes are found to be similar. The influence of the clamping strength was also considered. It was found that releasing and re-clamping did not have a significant effect on the natural frequencies of the structures. The smart sensing method can detect damage corresponding to 0.1 % changes in mass of the structure.

Work in progress includes the characterization of damage position.

ACKNOWLEDGEMENTS

This research was funded in part by the National Aeronautics and Space Administration and in part by the U.S. Air Force Office of Scientific Research under grant 49620-95-1-0236. The authors would like to thank Dr. William Winfree, NESB, NASA Langley Research Center and Dr. Yun Wang, while at the Mathematics Products Division, Brooks AFB, for numerous helpful discussions.

REFERENCES

1. H.T. Banks, P. Emeric and L. Plancke, *Modeling of Non-Symmetrical Damage in Plate-Like Structures,* to appear in Mathematical and Computer Modelling, Pergamon.
2. *Smart Structures and Materials 1995: Mathematics and Control in Smart Structures.* Vasundara V. Varadan, Editor. Proc. SPIE 2442, 1995.

3. L. Keyu, *NDT Solution: Interferometric Smart Material for Measuring Permanent Deformations,* Materials Evaluation, vol. 54 n. 5 p. 561, 1996.
4. H.T. Banks, D.J. Inman, D.J. Leo and Y. Wang, *An Experimentally Validated Damage Detection Theory in Smart Structures*, NC State University, CRSC-TR95-7, 1995; J. of Sound and Vibration, n. 191 (1996), pp. 859-880.
5. H.T. Banks, P. Emeric and L. Plancke, *Modeling of Non-Symmetrical Damage in Plate-Like Structures,* NC State University, CRSC-TR97-12, 1997.
6. J. Zelenka, *Piezoelectric Resonators and their Applications,* Elsevier, 1986.
7. Nellya N. Rogacheva, *The Theory of Piezoelectric Shells and Plates,* CRC Press 1994.
8. H.T Banks, R.C. Smith and Y. Wang, *Smart Material Structures: Modeling, Estimation and Control,* Masson/J. Wiley, Paris, Chischester, 1996.